Analysis of a scanning pentaprism system for measurements of large flat mirrors

Julius Yellowhair[1,*] and James H. Burge[2]

[1]Currently with Sandia National Laboratories, 1515 Eubank SE, Albuquerque, New Mexico 87123, USA
[2]College of Optical Sciences, University of Arizona, 1630 East University Boulevard, Tucson, Arizona 85721, USA

*Corresponding author: jeyello@sandia.gov

Received 22 February 2007; revised 26 July 2007; accepted 29 July 2007;
posted 8 August 2007 (Doc. ID 80354); published 3 December 2007

The optical surface of a large optical flat can be measured using an autocollimator and scanning pentaprism system. The autocollimator measures the slope difference between a point on the mirror and a reference point. Such a system was built and previously operated at the University of Arizona. We discuss refinements that were made to the hardware, the alignment procedure, and the error analysis. The improved system was demonstrated with a 1.6 m flat mirror, which was measured to be flat to 12 nm rms. The uncertainty in the measurement is only 9 nm rms. © 2007 Optical Society of America

OCIS codes: 120.3940, 220.4840.

1. Introduction

In optical surface metrology, systems with pentaprism(s) are used where conventional interferometric testing would otherwise be difficult or limited [1–4]. Two commonly used methods for testing flat mirrors interferometrically are the Fizeau [5] and Ritchey–Common [6] tests. The Fizeau test uses mostly commercial Fizeau interferometers, which are generally limited to 10 cm apertures. Thus commercial Fizeau interferometers are insufficient for full surface testing of large flat mirrors without performing subaperture testing and stitching. The accuracy and efficiency of the measurements diminish as the subaperture becomes smaller compared to the size of the test surface. The Ritchey–Common test can measure full flat surfaces, but the test requires a reference spherical mirror larger in size than the flat mirror under test. On a large scale this test is difficult and cumbersome to set up. The scanning pentaprism test overcomes these limitations and can measure low order aberrations on any large flat mirror.

In this paper we describe and analyze the scanning pentaprism test, a highly accurate optical slope test, to measure flatness in very large mirrors. The main components of the test system are two pentaprisms and a high resolution electronic autocollimator. The test system builds on a previous scanning system, which was designed to deflect the autocollimator beam up to a flat mirror suspended above the test site [1,2]. In contrast, our refined system deflects the beam down to where the large flat mirror is supported on a polishing table and whiffletree-type support. We use a second autocollimator as part of an active feedback control to maintain angular alignment of one prism during scanning operation. The main improvements to the previous system are in the mechanical hardware to provide more stability and to maintain alignments during scanning, an alignment procedure to increase the accuracy of the system, and error analysis to help establish the system performance. The system performance is only limited in accuracy by second order error influences due to coupling between misalignments and motions in the autocollimator, prisms, and the test surface. Beam errors also couple with lateral motion of the scanning prism to cause additional second order slope errors. The refinements to the system help minimize these errors. We provide an error analysis to quantify the measurement errors. Using the results from the error analysis, we show through Monte Carlo simulations that over a 2 m flat the accuracy for measur-

0003-6935/07/358466-09$15.00/0

ing power is about 9 nm rms with the improved system.

Pentaprisms deflect light beams at a constant angle (nominally by 90°) regardless of its orientation in the line-of-sight direction. Various optical test systems and devices involving pentaprisms make use of this unique property. Systems involving pentaprisms have been developed to measure optical surface errors by measuring surface slopes [1–4]. Simply integrating the slope data gives surface height profiles. Through multiple measurements of the optical surface in different directions, a full synthetic surface map can be obtained. Other systems with pentaprisms are used to aid in optical alignments or to make low order error corrections to deformable optical surfaces. Sensitive optical alignments and error corrections are made possible by the capability of multiple pentaprisms to project collimated and nominally parallel reference beams onto optical surfaces. Due to the usefulness of pentaprism systems, efforts have been made to understand the error influences and build systems that are less sensitive to alignment and motion errors [7,8].

2. System Design and Development

A. Test Concept

In this subsection we discuss the test concept and design of the scanning pentaprism system. A schematic diagram of the test setup is shown in Fig. 1. Two pentaprisms were coaligned to a high resolution electronic autocollimator. Both prisms deflected the collimated beam from the autocollimator nominally by 90° to the mirror surface. The first prism had a coupling wedge that transmitted about 50% of the beam to the second prism. The beams reflected off the test surface and returned to the autocollimator, where small angle deviations revealed slope errors in the mirror surface.

The test system can be used in either a scanning or a nonscanning mode. In the scanning mode, the first (reference) prism remained fixed, while the second (scanning) prism was translated over the mirror surface sampling the mirror every few centimeters. Since the autocollimator can only measure one return signal at a time, we used electronically controlled shutters to alternately select the reference path and the scanning path. By taking a difference between the two prisms, the measurements became insensitive to the motions of the autocollimator and test mirror in the measurement direction. An integration of the slope data provided surface height profiles along the scanning direction. We used an alternative method of fitting low order slope functions derived from the Zernike polynomials to the slope data through a least squares calculation [9]. We determined the Zernike coefficients after the fit and reconstructed a surface topology map using slope data from several scans at different orientations over the mirror. In the nonscanning or staring mode, both prisms remained fixed, and the flat mirror under test was rotated while the slope data were acquired continuously. Typically, we positioned the reference prism at the edge of the mirror and the scanning prism at the center of the mirror. The nonscanning mode measured θ dependent aberrations such as astigmatism (2θ dependence) and trefoil (3θ dependence). In Section 3, we provide results from both modes of operation.

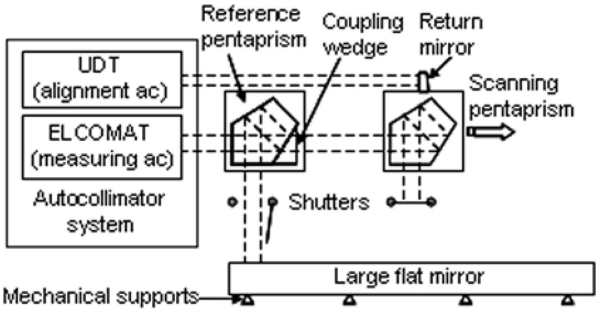

Fig. 1. Schematic of the scanning pentaprism test system.

The pentaprism system allowed slope determination only in the scan or measurement direction. We call this direction the line-of-sight pitch or in-scan direction. The degrees of freedom (pitch, yaw, and roll) for the main test components are defined in Fig. 2. Coupling between misalignments and motions of the components in these degrees of freedom caused second order errors to the beam line of sight. Sources of line-of-sight errors up to second order are listed in Table 1. The line-of-sight pitch (scan direction) varies linearly with autocollimator and test surface pitch angles, and quadratically with other angular parameters. The first order error from the autocollimator and test surface pitch motions were common to both prisms, so these errors were eliminated by performing difference measurements between the two prisms. Careful system alignment and active control of the scanning prism minimized the second order errors.

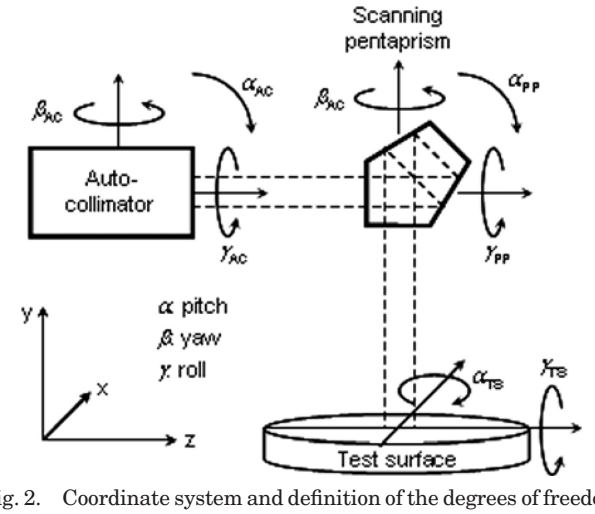

Fig. 2. Coordinate system and definition of the degrees of freedom for the autocollimator, scanning pentaprism, and test surface.

Table 1. Contributions to Line-of-Sight Error

Contributions to Line-of-Sight Pitch (In-Scan Direction)	Contributions to Line-of-Sight Roll (Cross-Scan Direction)
α_{AC}	β_{AC}
α_{TS}	β_{PP}
γ_{PP}^2	γ_{PP}
$\gamma_{AC} \times \gamma_{PP}$	γ_{TS}
$\gamma_{AC} \times \beta_{PP}$	$\alpha_{AC} \times \beta_{PP}$
$\gamma_{AC} \times \gamma_{TS}$	$\alpha_{AC} \times \beta_{TS}$
$\gamma_{TS} \times \gamma_{PP}$	$\alpha_{AC} \times \gamma_{AC}$
$\gamma_{TS} \times \beta_{PP}$	$\alpha_{AC} \times \gamma_{PP}$
α: pitch	AC: autocollimator
β: yaw	PP: pentaprism
γ: roll	TS: test surface

1. Pentaprism Pitch Motion Sensitivity

Small pitch motion of the pentaprism was expected. This motion, however, had no effect on the beam deviation in the line-of-sight pitch direction. This is the beauty of the pentaprism: the input beam is deviated at a constant (nominally) 90° angle, independent of small pitch errors. We took full advantage of this unique property.

2. Pentaprism Yaw and Roll Motion Sensitivities

The in-scan (vertical) and cross-scan (horizontal) angles, as seen by the autocollimator, were coupled for pentaprism yaw and roll motions. The dependence is linear for prism yaw motion and quadratic for roll motion [7,8]. When the prism was aligned, the spot motion was the same for small prism roll and yaw motions. The in-scan measurement was then perpendicular to the spot motion caused by motions in prism roll and yaw. The noise over the amount of motion in roll and yaw gave the accuracy of the alignment. For example, if the prism yaw and roll alignments were maintained to 50 μrad, the in-scan measurements varied by less than 10 nrad (discussed in Section 4).

Information from the pentaprism yaw motion can be used to align both the autocollimator roll and the prism roll. Geckeler [8] derives the slope of the autocollimator angle readings (vertical angle versus horizontal angle) from the pentaprism yaw scan as

$$M_{\text{scan}}^{\text{yaw}} = \alpha_{TS} - \alpha_{AC}, \quad (1)$$

which reveals information on the difference of the roll angles of the autocollimator and the test surface. The autocollimator roll was aligned relative to the test surface when the slope, M, became zero. In addition, Geckeler [8] derives the minimum of the parabola from the pentaprism roll scan (vertical angle versus horizontal angle) as

$$H_{\text{scan}}^{\text{roll}} = \beta_{PP} - \beta_{AC} + 0.5 M_{\text{scan}}^{\text{yaw}}, \quad (2)$$

which depends on the pentaprism and autocollimator yaw and the result of the yaw scan. Both Eqs. (1) and (2) have dependence on pentaprism yaw; thus prism yaw can be used to align autocollimator roll [from Eq. (1)] and prism roll [from Eq. (2)].

3. Beam Collimation Errors and Alignment to the Prism Motion

The errors in the autocollimator collimated beam coupled with lateral pentaprism motion to cause additional second order slope errors. We estimated that this effect caused 280 nrad slope change per 1 mm of lateral prism motion. This linear motion of the scanning prism was aligned to less than 0.5 mm along the beam, so the above effect was limited to 140 nrad surface slope variation (discussed in Section 4).

B. System Hardware

In this subsection, we describe the components of the system. This includes the mechanical and optical hardware and measurement units.

1. Optical Rails

A major improvement in stability over the previous system was in the mechanical stage used for the scanning operation. The new rail system consisted of two 2.5 m heavy duty steel rails spaced 20 cm apart and bridged by the pentaprism and autocollimator platforms as shown in Fig. 3. The straightness of the rail system was measured with a laser tracker to better than 0.05 mm/m, a significant improvement over the previous rail system. Thus the advantage of the new rails was that they limited the lateral and angular motion of the scanning prism, resulting in less reliance on the active control system. In addition, the new rails were less susceptible to vibrations and warping; vibrations and warping were notable drawbacks of the previous rails. The new rails and the active control system maintained the alignment of the pentaprisms to within 50 μrad in roll and yaw. The new rails rested on a three point kinematic base. The kinematic base allowed the test system to be removed and stowed when not in use.

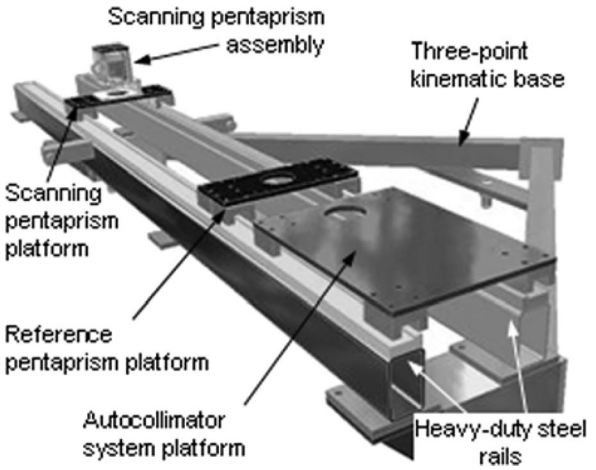

Fig. 3. Solid model of the scanning pentaprism rail system showing the mounting platforms and the three-point kinematic base.

2. Autocollimators

We used two electronic autocollimators. The first was a high resolution autocollimator (Elcomat 2000 made by Moller–Wedel) used for the surface slope measurements. The Elcomat 2000 provided a 40 mm collimated beam, which was projected onto the mirror surface using the two pentaprisms (as described previously). The reflected beam from the scanning prism was detected by the Elcomat, and angle deviations caused by slope variations in the mirror surface were measured. The Elcomat also functioned as part of the active control system that monitored cross-scan beam motion due to prism roll or yaw motion.

The second autocollimator had less angular resolution (model 3700 made by United Detector Technologies). The UDT 3700 autocollimator was aligned to a return flat mirror that was attached to the scanning pentaprism assembly (see Fig. 1). The UDT autocollimator was the main component of the active control used to monitor the yaw motions of the scanning pentaprism. The UDT autocollimator was insensitive to roll motion of the pentaprism, but the Elcomat sensed the line-of-sight roll, which was caused by a combination of the prism roll and yaw motions. The prism roll was determined as the difference between the line-of-sight roll and the prism yaw motion. The UDT autocollimator decoupled the two prism motions for the Elcomat. The active control was then programmed to maintain both the roll and yaw alignments of the scanning prism to 50 μrad.

3. Pentaprisms and Holders

The first pentaprism had a coupling wedge that allowed about 50% transmission of the beam to the second pentaprism as shown schematically in Fig. 1. We estimated measuring through the first prism with the wedge caused about 50 nrad rms measurement errors in the scanning mode (see Section 4).

The prism holders provided secure mounts and remote adjustment of prism yaw and roll motions through Picomotor (New Focus) linear actuators (see Fig. 4). The Picomotor actuators were controlled through the active control system; any misalignments of the prisms during scanning were fixed by sending commands to the Picomotors to drive the prisms back into alignment. The prism assemblies were mounted on rail cars, which moved on the two parallel steel rails.

4. Shutters

We used two electronically controlled shutters, which were mounted between the pentaprisms and the test mirror as shown in Fig. 4 or schematically in Fig. 1. The shutters allowed alternating measurements between the prisms. Shutter A was open and shutter B closed when measuring through the reference prism occurred. The shutter states were reversed when measuring through the scanning prism occurred. A few seconds delay between shutter operation and measurement allowed vibrations caused by the shutters to damp out.

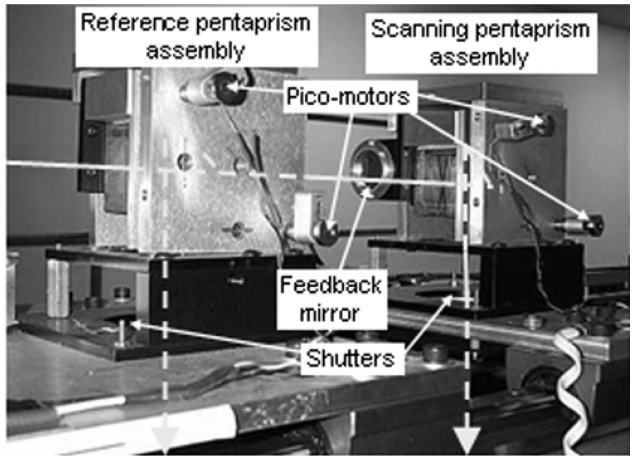

Fig. 4. Pentaprism assemblies integrated into the system. Electronically controlled shutters are located at the exit face of each prism. The autocollimator system (not visible) is mounted to the left.

C. System Integration

The system can be thought of as an assembly of subsystems, which included the autocollimator system, the reference and scanning pentaprism assemblies, and the electronics including the workstation and software for active control.

The rail system was the foundation upon which these subsystems were integrated (see Fig. 5). The autocollimator system and prism assemblies were mounted on carriage platforms that were attached to rail cars. The platforms then moved on the rail tracks; however, only the scanning prism assembly was allowed to translate over the rails. The autocollimator system and the reference prism assembly were locked into position at one end of the rails. The electronics and cabling for the active control were housed in a breakout box and mounted underneath the autocollimator system platform (not visible in Fig. 5). The fully integrated system is shown in Fig. 5. The entire system weighed about 200 kg and could be lifted with a hoist and positioned kinematically over the large mirror.

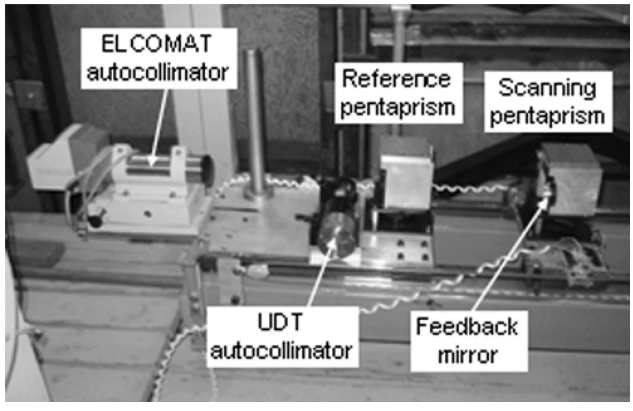

Fig. 5. Fully integrated and operational scanning pentaprism test system.

D. System Alignment

Accurate system alignment is essential to slope measurement accuracy [7,8]. The system alignment was performed in several steps described below, starting with the coarse and then the fine alignment.

(1) The large flat mirror rested on a whiffletree-type support and an air bearing polishing table, which was leveled to gravity. The pentaprism rails were also leveled to gravity; thus tilt between the test surface and the rails was minimized from the beginning.

(2) A standard He–Ne laser was mounted in place of the measuring autocollimator. The laser was aligned to the rails by placing a cross-hair target on the scanning pentaprism assembly, then by pointing the laser at the cross-hair while sliding the prism assembly back and forth over the rails. After the laser was aligned to the rails to less than 0.25 mm/m, the scanning prism was parked at the furthest point on the rails opposite the reference prism.

(3) The cross-hair target was removed, and the laser was reflected off the prism front faces. Both prisms were adjusted in yaw until the laser returned through a 2 mm pinhole placed in the laser path (see Fig. 6). This initial alignment of the prisms in yaw was better than 120 μrad with respect to the measurement direction.

(4) The roll motion of the reference prism was aligned by opening the shutter, reflecting the laser beam off the test mirror, and adjusting the roll of the prism until the reflected laser spot returned through the pinhole. The procedure was repeated for the scanning prism. At this point the initial alignment of prism roll was also better than 120 μrad with respect to the measurement direction.

(5) Next, a return flat mirror (5 cm diameter) was placed in the path of the laser beam just before the scanning prism. The return mirror was secured and adjusted until the reflected laser beam returned through the pinhole. The laser and the pinhole were removed, and the measuring autocollimator was put in place. The autocollimator was aligned to the return mirror in both the horizontal and vertical axes. At this point the autocollimator was aligned to the rail and the prisms to better than 120 μrad.

(6) The fine alignment was performed iteratively using the readout of the autocollimator. While the test surface remained fixed, typically adjustments were made to the autocollimator and the prisms. Table 1 lists the angular motions that affected the beam line-of-sight pointing (pentaprism yaw and roll and autocollimator roll). These are the motions that required adjustments to achieve optimal system alignment. First, the scanning prism was scanned in yaw by about ±200 μrad, and the autocollimator horizontal and vertical angle readings were observed. The behavior of this motion is linear on the angle readings. A finite slope in the angle readings indicated a misalignment between the autocollimator and test surface in roll. With the test surface fixed, adjustment was made to the autocollimator to minimize this misalignment. After adjusting the roll of the autocollimator, the prism was rescanned in yaw. Roll of the autocollimator was aligned when the angle readings were no longer coupled for the prism yaw scan. The autocollimator roll was now aligned to better than 50 μrad.

(7) Next, the reference prism was scanned in roll by about ±200 μrad, and the autocollimator horizontal and vertical angle readings were observed. The behavior of this motion is quadratic on the angle readings. Any coupled readings over small prism roll motion indicated a misalignment of the prism in yaw. Yaw of the prism was adjusted, and the prism was then rescanned in roll. The prism yaw was aligned when no noticeable coupling remained between the angle readings during the roll scans. The roll motion was now constrained to the vicinity of the quadratic minimum. This procedure was repeated for the scanning prism. Yaw and roll for both prisms were now aligned to better than 50 μrad. The system was now aligned and ready to use.

3. System Performance

The scanning pentaprism system can be used in two modes: scanning or staring (nonscanning). Diagonal surface scans were performed in the scanning mode (see Fig. 7). In the staring mode, circumferential scans were performed where both prisms remained fixed and the test flat rotated continuously while data were acquired (see Fig. 11).

A. Diagonal Line Scans in Scanning Mode

In the scanning mode, the reference pentaprism remained fixed and the scanning prism was translated across the diameter of the mirror acquiring a measurement every few centimeters. Typically, we sampled the 1.6 m flat with 25 to 50 points across with higher measurement density near the edges to monitor the edges during fabrication. A diagram showing

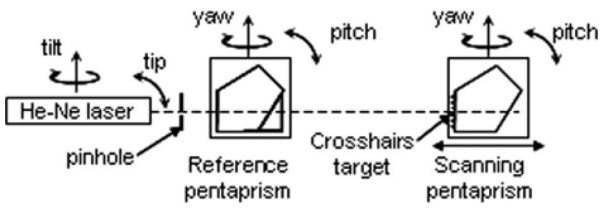

Fig. 6. Initial alignment of the pentaprisms in yaw. The laser is reflected off the front faces of the prisms.

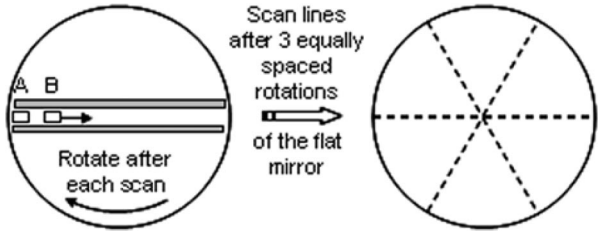

Fig. 7. Pentaprism scan arrangement. This example shows the mirror being rotated in 120° steps for each scan.

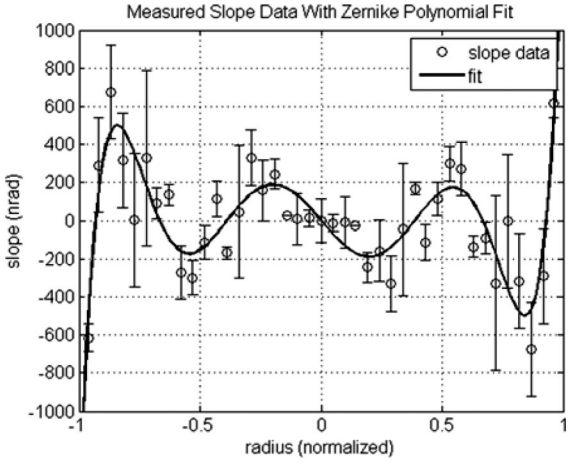

Fig. 8. Surface slope measurements with the scanning pentaprism system and a low order polynomial fit. A linear component of the polynomial fit on the slope data gives information on power in the surface (12 nm rms).

an example of three scan paths is shown in Fig. 7. This was achieved by rotating the test flat to two other positions after the first scan. The three line scans measured the low order Zernike aberrations [9].

A single diagonal line scan measured only rotationally symmetric aberrations. Figure 8 shows the result of a single diagonal line scan on the finished 1.6 m flat mirror. Forward and backward scans were performed for the same diagonal line, and the data were averaged. Only the slope functions from the symmetric Zernike polynomials were fit to the slope data. The linear component of the polynomial fit to the slope data then revealed power in the mirror surface. This measurement yielded 12 nm rms in power.

A radially normalized plot showing the scanning pentaprism slope data in comparison to the Fizeau interferometer data for the finished 1.6 m flat is shown in Fig. 9. The figure shows that the scanning pentaprism data and interferometer data, first differentiated to obtain the surface slope, have no significant differences, except at the very edge where high

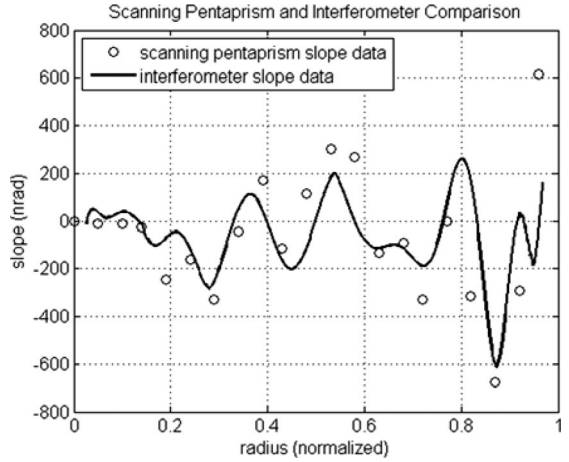

Fig. 9. Comparison of the scanning pentaprism slope data and the interferometer slope data.

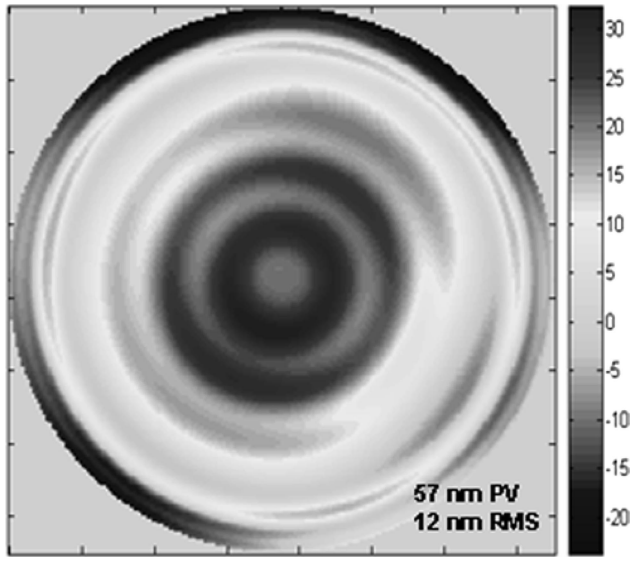

Fig. 10. Interferometer measurement on the 1.6 m flat mirror.

slopes were observed. The rms difference is about 160 nrad after removing the edge point, which is within the accuracy (see Section 4) of the scanning pentaprism test in the scanning mode. The large Fizeau interferometer did not measure power, so the interferometer data were adjusted for power before the comparison. The Fizeau interferometer used a 1 m custom reference flat and subaperture testing to measure the 1.6 m flat mirror (Figs. 10 and 11). The surface map, shown in Fig. 11, is from the finished mirror after combining the subaperture measurements. The surface map, measured to 12 nm rms, shows mostly zonal errors.

B. Circumferential Scans: Staring Mode

The circumferential scans provided information on θ dependent aberrations such as astigmatism (2θ) and trefoil (3θ). Tilt between the autocollimator and the test surface had a 1θ dependence. The main aberration measured in this mode was astigmatism.

In the circumferential scans, both pentaprisms were fixed and the flat mirror was continuously rotated (see Fig. 11). The slope data were continuously acquired for several full rotations of the flat mirror. The data were then averaged.

For the scans shown in Fig. 12(a), the reference pentaprism (A) was parked near the edge of the large

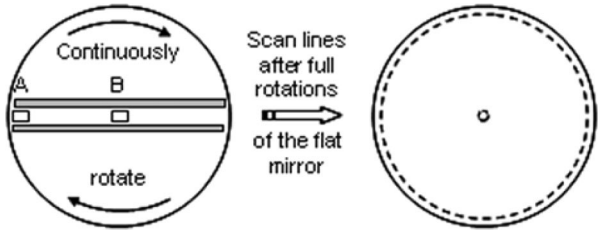

Fig. 11. Circumferential scans, where both prisms are fixed and the mirror is continuously rotated, measure astigmatism, and other θ dependent aberrations in the mirror surface.

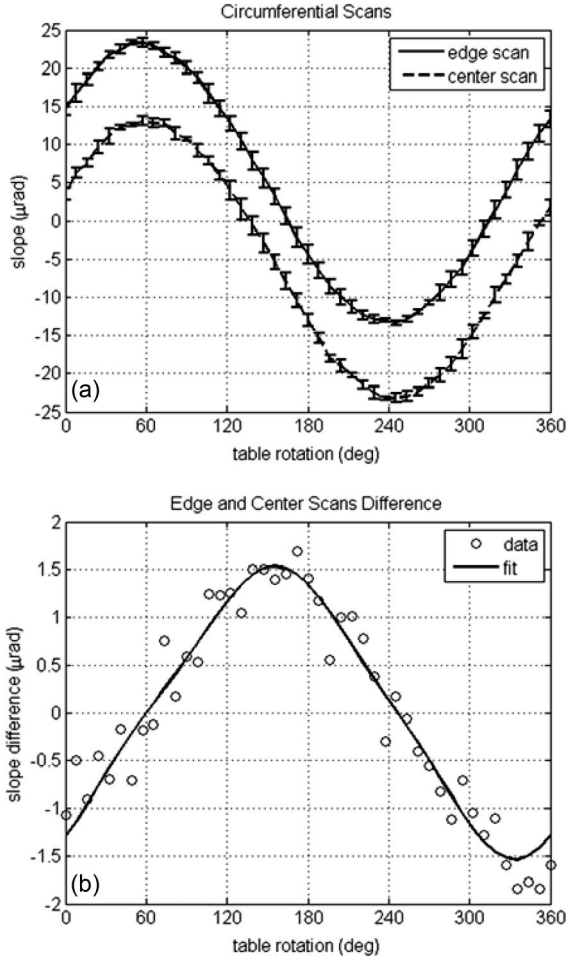

Fig. 12. (a) Circumferential scans at the center and edge of the large flat mirror, and (b) difference in the center and edge scans and curve fit. The error bars in the scans indicate stability of the rotary air bearing table.

flat mirror, and the scanning pentaprism (B) was parked at the center of the mirror. These measurements were performed while the mirror was in production. The difference between the scans [Fig. 12(b)] reveals the amount of contributions of low order θ dependent aberrations (dominated by tilt).

A least squares fit of the difference data was performed using a fitting function of the form

$$f = a_0 + a_1 \sin(\theta) + b_1 \cos(\theta) + a_2 \sin(2\theta) + b_2 \cos(2\theta) + a_3 \sin(3\theta) + b_3 \cos(3\theta). \quad (3)$$

Table 2 lists the θ dependent aberrations and their coefficient values after the fit. The last column shows the equivalent surface error for each θ dependent aberration.

4. Error Analysis

A. Errors to Line-of-Sight Beam Motion

There were several error sources that contributed to the line-of-sight beam pitch (or in-scan) motion. Below, we describe the error sources and quantify their effect on the beam line of sight.

1. Errors from Angular Motions of the Pentaprisms and Autocollimator

Taking the second order terms from Table 1, an expression for the change in the in-scan line of sight due to misalignments and angular motions of the autocollimator, pentaprism, and test surface can be derived as

$$\Delta\alpha_{LOS} = 2\gamma_{PP} \times \Delta\gamma_{PP} + \Delta\gamma_{AC}(\gamma_{PP} + \beta_{PP} + \gamma_{TS}) + \gamma_{AC}(\Delta\gamma_{PP} + \Delta\beta_{PP} + \Delta\gamma_{PP}) + \Delta\gamma_{TS}(\gamma_{PP} + \beta_{PP}) + \gamma_{TS}(\Delta\gamma_{PP} + \Delta\beta_{PP}), \quad (4)$$

where each Δ term indicates the variation in autocollimator, prism, and test surface motions for that angle. Equation (4) shows that the motions of the three components couple with misalignments to cause second order slope errors in the in-scan line of sight. Table 3 shows a summary of the error terms that coupled into the measurement in the in-scan direction, and Table 4 shows the amount of contribution from each error term in Eq. (4).

2. Mapping Error

The slope errors in the polished test surface were expected to be less than 2 nrad/mm rms. The position of the scanning prism (or the beam) on the test surface was known to 2 mm. The error due to the prism position thus contributed less than 4 nrad rms to the total error.

3. Thermal Errors

The pentaprisms were made from BK7 glass, which is fairly sensitive to temperature gradients (7.1×10^{-6}/°C). A linear temperature gradient in the prisms changed the index gradient and prism geometry. The thermal analysis showed that a temperature gradient of 0.01 °C/m in the prisms would cause an additional beam deflection in the line-of-sight direction of 17 nrad. The time scale for the two modes of operation of the test system was relatively short compared to the prisms' thermal time constant. In the scanning mode we estimated a single scan took

Table 2. Aberrations Measured with Circumferential Scans

Aberration Term	Fit Function Term(s)	Fit Coefficients (μrad)	Equivalent Low-Order Surface Error
Piston	a_0	0.0294	—
Tilt	$a_1 \sin(\theta) + b_1 \cos(\theta)$	0.6328, −1.2888	359 nm rms
Astigmatism	$a_2 \sin(2\theta) + b_2 \cos(2\theta)$	0.0366, −0.0043	15 nm rms
Trefoil	$a_3 \sin(3\theta) + b_3 \cos(3\theta)$	0.0993, −0.0283	18 nm rms

Table 3. Budget for Alignment Errors for the Pentaprism/Autocollimator System

Parameter	Description	Tolerance
γ_{PP}	Initial misalignment of the prism roll	<0.13 mrad
$\Delta\gamma_{PP}$	Variation in prism roll	<0.05 mrad rms
γ_{AC}	Misalignment of the autocollimator roll relative to direction of motion	<0.10 mrad
$\Delta\gamma_{AC}$	Variation in autocollimator roll	<0.05 mrad rms
β_{PP}	Initial misalignment of the prism yaw	<0.13 mrad
$\Delta\beta_{PP}$	Variation in prism yaw	<0.05 mrad rms
γ_{TS}	Misalignment of the test surface roll relative to the direction of motion	<0.10 mrad
$\Delta\gamma_{TS}$	Variation in test surface roll	<0.01 mrad rms

one hour. For a full measurement, three scans were performed that required about three hours to complete. In the staring mode, a full measurement typically lasted 10 to 15 min. Only the variation in temperature gradients during the three hour scan in scanning mode and 15 min scan in staring mode contributed to the line-of-sight errors. The top level error budget allowed for change in the thermal gradient of ± 0.04 °C/m for the scanning case and ± 0.02 °C/m for the staring case. We then expected a line-of-sight error of up to 34 nrad rms and 17 nrad rms for scanning and staring cases, respectively.

4. Errors from Coupling Lateral Motion of the Pentaprisms

Phase or amplitude variations in the collimated beam did not affect the system performance to first order, because these effects were common to both pentaprisms. These variations and other beam errors, however, coupled with lateral motion of the scanning prism (relative to the collimated beam) to cause second order errors. Coupling of phase errors, diffraction effects, beam nonuniformity, and prism errors with lateral motion of the prisms for the scanning system was analyzed by Mallik *et al.* [1,2]. This analysis for our system is not repeated here; our system had better control of the lateral motion of the prisms. The lateral motion of the scanning prism in our system was aligned and maintained to 0.5 mm. The combined effect of these errors was then estimated to be less than 80 nrad rms.

Table 4. Misalignment and Perturbation Influences on the Line of Sight

Contribution (Terms from Eq. (4))	Amount of Line-of-Sight Deviation (nrad rms)
$2\gamma_{PP} \times \Delta\gamma_{PP}$	13
$\Delta\gamma_{AC} \times \gamma_{PP}$	7
$\Delta\gamma_{AC} \times \beta_{PP}$	7
$\Delta\gamma_{AC} \times \gamma_{TS}$	5
$\gamma_{AC} \times \Delta\gamma_{PP}$	5
$\gamma_{AC} \times \Delta\beta_{PP}$	5
$\gamma_{AC} \times \Delta\gamma_{TS}$	1
$\Delta\gamma_{TS} \times \gamma_{PP}$	1
$\Delta\gamma_{TS} \times \beta_{PP}$	1
$\gamma_{TS} \times \Delta\gamma_{PP}$	5
$\gamma_{TS} \times \Delta\beta_{PP}$	5
Root sum square	20

Table 5. Independent Measurement Errors Assumed to be Uncorrelated

Error Description	Staring Mode (nrad rms)	Scanning Mode (nrad rms)
Autocollimator measurement uncertainty (range dependent)[a]	140	160
Prism and beam angle variation	20	20
Mapping error	4	4
Thermal effects	17	34
Effect of reference prism error	25	50
Coupling of lateral motion	—	80
Root sum square	145	190

[a]Manufacture's specification.

5. Combined Random Errors

Table 5 shows the random errors for the pentaprism staring and scanning modes separately. There was an additional error in acquiring the measurements from the scanning pentaprism through the fixed reference pentaprism. This effect is included directly in Table 5.

6. Analysis of Errors Due to Beam Divergence

There is an additional error to consider that coupled into lateral motion of the pentaprism. For typical uses of electronic autocollimators, a collimated output beam is assumed. If the beam is slightly diverging, however, the angle readings are shifted by some amount proportional to the divergence angle. In the scanning pentaprism system, this effect of the beam divergence can couple into lateral motion of the pentaprism causing a second order error. To quantify this effect, we devised a simple test. A 13 mm circular aperture was placed at the output port of the measuring autocollimator. The aperture was shifted up and down perpendicular to the line of sight by about 18 mm from the top edge of the beam to the bottom

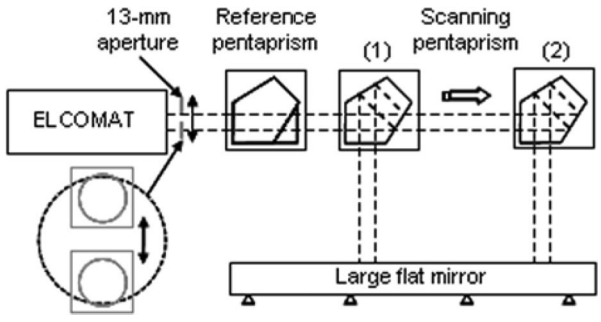

Fig. 13. Setup to test for the effect of beam divergence on prism motion.

Table 6. Measurement Accuracy for the Low-Order Zernike Aberrations with the Scanning Pentaprism System

Zernike Aberration	Measurement Accuracy (nm rms)
Power	9
Cos astigmatism	8
Sin astigmatism	8
Cos coma	4
Sin coma	4
Spherical	2
Secondary spherical	2
Root sum square	16

edge as shown in Fig. 13, and the change in the vertical angle reading was recorded for the two aperture positions.

For the case when the scanning prism was close to the reference prism [1], the change in the autocollimator vertical angle reading was about 10 μrad. The scanning prism was then moved to the far edge of the flat mirror [2], and performed the aperture shifts. For this case, the change in the vertical angle reading was about 15 μrad. From these measurements we estimated that this effect caused about 280 nrad slope change per 1 mm of lateral motion. The prism linear motion was aligned to less than 0.5 mm along the beam, so the effect was limited to 140 nrad surface slope variation. This systematic slope variation of ±70 nrad corresponds to surface power of less than 8 nm rms.

B. Monte Carlo Simulation of the System Performance

A Monte Carlo simulation on the three diagonal surface scans separated by 120° was performed to determine the uncertainty distributions of the low order Zernike aberrations using a noise value of 0.3 μrad for a single differential measurement and assuming 42 measurement points per scan. The measurement uncertainty of each of the low order aberrations from the simulation is listed in Table 6. The simulation result shows that a 2 m flat mirror can be measured to 16 nm rms of low order aberrations with the scanning pentaprism system after careful system alignment. The measurement of power has 8 nm rms due to the systematic effect listed above, limiting the surface power measurement to 9 nm rms.

5. Conclusion and Future Work

We provided an analysis of a refined scanning pentaprism system that measured flatness in large flat mirrors to an accuracy of 9 nm rms; the system has the option to measure other low order aberrations and only θ dependent aberrations. The system alignment procedure was provided in detail. The measurement accuracy was limited only by second order influences from misalignments and autocollimator, pentaprism, and test surface motions, which were minimized through careful system alignment and active pentaprism motion control. A Monte Carlo simulation of the system performance was performed based on the measurement uncertainty estimated from the error analysis. The simulation result showed the uncertainty in the measured low order Zernike aberrations, and measurements to 16 nm rms of low order aberrations are achievable for 2 m flat mirrors. The high accuracy of the test system makes it ideal for absolute testing of arbitrarily large flat mirrors. This test system can be used as a final test on the surface figure or to guide polishing during fabrication. The kinematic base allows the test system to be moved to the polishing table without moving the test flat to a testing fixture and stowed during polishing or when not in use.

Absolute calibration of the system was not performed. This can be accomplished using a liquid reference surface over very long test paths (e.g., 4 m), where the liquid surface is only limited by the curvature of the earth. The result will be excellent characterization of the system performance. This task was left open for future work.

References

1. P. Mallik, C. Zhao, and J. H. Burge, "Measurement of a 2-m flat using a pentaprism scanning system," Opt. Eng. **46,** 023602 (2007).
2. S. Qian, P. Takacs, G. Sostero, and D. Cocco, "Portable long trace profiler: concept and solution," Rev. Sci. Instrum. **72,** 3198–3204 (2001).
3. S. Qian, W. Jark, and P. Z. Takacs, "The penta-prism LTP: a long-trace-profiler with stationary optical head and moving penta prism," Rev. Sci. Instrum. **66,** 2562–2569 (1995).
4. R. D. Geckeler, "ESAD shearing deflectometry: potential for synchrotron beamline metrology," Proc. SPIE **6317,** 63171H (2006).
5. M. V. Mantravadi, "Newton, Fizeau, and Haidinger interferometers," in *Optical Shop Testing,* D. Malacara, ed. (Wiley, 1992), pp. 1–49.
6. J. Ojeda-Castaneda, "Foucault, wire, and phase modulation tests," in *Optical Shop Testing,* D. Malacara, ed. (Wiley, 1992), pp. 265–320.
7. R. D. Geckeler, "Error minimization in high-accuracy scanning deflectometry," Proc. SPIE **6293,** 62930O (2006).
8. R. D. Geckeler, "Optimal use of pentaprisms in highly accurate deflectometric scanning," Meas. Sci. Technol. **18,** 115–125 (2006).
9. J. Yellowhair and J. H. Burge, "Measurement of optical flatness using electronic levels," Opt. Eng. (to be published).
10. J. Yellowhair, College of Optical Sciences, University of Arizona, 1630 East University Boulevard, Tucson, AZ 85721, R. Sprowl, P. Su, R. Stone, and J. H. Burge are preparing a manuscript to be called "Development of a 1 meter vibration-insensitive Fizeau interferometer."